Poroelasticity of saturated solids with an application to blood perfusion

Pergamon

PII: S0020-7225(96)00009-2

Int. J. Engng Sci. Vol. 34, No. 9, pp. 1019–1031, 1996

0020-7225/96 $15.00 + 0.00

POROELASTICITY OF SATURATED SOLIDS WITH AN APPLICATION TO BLOOD PERFUSION

W. J. VANKAN†, J. M. HUYGHE‡, J. D. JANSSEN‡ and A. HUSON‡
Department of Mechanical Engineering, Eindhoven University of Technology, The Netherlands

Abstract—A description of finite deformation of, and fluid flow through, a hierarchically arranged porous solid has been developed using the theory of mixtures. This hierarchical mixture consists of one solid constituent and a fluid constituent that is subdivided into a continuous series of intercommunicating compartments. Conservation laws for mass and momentum have been derived and appropriate formulations for the constitutive behaviour of the constituents are proposed. A finite element description of the hierarchical mixture model has been implemented in the software package DIANA. Two-dimensional, axisymmetric and three-dimensional elements can be used in finite deformation analysis. An example of application is blood perfused biological tissue. A simulation of a blood perfused contracting skeletal muscle is presented. Copyright © 1996 Elsevier Science Ltd

1. INTRODUCTION

The mixture theory has proven to be a valuable means to model the mechanical behaviour of biological tissue [1–3]. In this theory the various solid and fluid components of the tissue are modelled as interacting continua. An important fluid component in biological tissue is blood. It is responsible for the nutrition and drainage processes that are essential for the tissue. Blood flows through a hierarchical system of blood vessels: the vascular tree. This tree consists of one or a few large arterial vessels from which smaller vessels bifurcate (Fig. 1) and diverge into numerous capillaries which assemble to converging venous vessels. Because of this hierarchical architecture blood flow cannot be adequately described by biphasic mixture theory: the state of the blood depends strongly on the position in the hierarchy. For example, the velocity and pressure of the capillary blood are much lower than of the arterial blood. The pressure difference between arterial and venous vessels is essential as the driving force for the blood flow. Huyghe *et al.* [4, 5] developed an extended form of Darcy's equation in which this dependency of the fluid flow on hierarchical position was included. They verified their model for Newtonian flow through a rigid vascular tree. Because in biological tissue alterations in blood perfusion can occur due to deformations of the tissue [6], the focus of this study is to integrate the concepts developed in [4] into a finite deformation theory of saturated porous media.

Aifantis [7] introduced the concept of multiporosity for deforming media that are characterized by several distinct families of diffusion or flow paths. A special case of this concept, in which only two degrees of diffusivity were included, was applied to fissured rock formations, in which most of the fluid volume is located in the low permeability pores of the rock, and most of the permeability is associated with the fissures [8]. An important aspect of blood perfused biological tissue, which is not covered by Aifantis' multiporosity concept, is the vessel wall, which can be regarded as an elastic interface between solid (tissue) and fluid (blood). In [9, 10] Huyghe and van Campen derived a description of finite deformation of hierarchical porous media, in which they used a formal averaging procedure. Unlike the previous authors, they included the concept of a vessel wall, and they derived an extended Darcy equation for the case of anisotropic orientation of the interface between compartments

†Address for correspondence: W. J. Vankan, University of Limburg, Department of Movement Sciences, P.O. Box 616, 6200 MD Maastricht, The Netherlands.
‡Also at the University of Limburg, Department of Movement Sciences, P.O. Box 616, 6200 MD Mastricht, The Netherlands.

Fig. 1. Scanning electron micrograph of a polymer cast of the arterial part of a vascular tree. A large supplying arterial vessel ($d \approx 0.5$ mm) can be observed, from which many smaller vessels bifurcate. The smallest vessels that were reached by the polymer are arterioles with diameters of about 50 μm. In reality, from these vessels smaller and smaller vessels bifurcate, with diameters down to 5 μm (capillaries), after which the converging venous bed is reached. The small white line on the lower right-hand side of the photograph represents a distance of 1 mm.

from the assumption of validity of a Poiseuille-type equation on the level of the individual pore. Moreover, they used a continuous spectrum of porosities.

In this paper, mixture theory is used to derive the same equations as presented in [9, 10], in a more general context of hierarchical porous media. The tissue is modelled as a mixture of one solid and one fluid where the fluid represents the blood. The fluid is subdivided into a number of compartments, each of which represents the blood on a different hierarchical position in the vascular tree. Blood flow through the vasculature is described as communication between the fluid compartments, which corresponds with the physiological definition of perfusion: the volume of blood passing a given level in the vascular hierarchy per unit of time and per volume of tissue. Vessel walls, modelled as an elastic solid–fluid interface, are included as a local contribution of the pressure difference between solid and fluid to the mixture's elastic energy. Although this mixture description is specifically developed for biological materials, its applicability to technical materials is not excluded.

In the derivation of the hierarchical mixture model conservation laws of mass and momentum have been formulated and corresponding constitutive behaviour has been derived from constitutive theory. An integrated finite element description of the total mixture model has been developed and implemented in the DIANA software package [11]. The implementation was subjected to several test procedures, one of which was comparison of the finite element solution with the analytical solution for a confined compression test. As an illustration of the possibilities of the model a simulation of contraction of a perfused skeletal muscle has been performed.

2. CONSERVATION LAWS

In the technical literature we find porous media theories dealing with solids saturated with different fluid constituents [12]. Bowen [13] has derived equations from mixture theory for ν incompressible immiscible fluids saturating one incompressible solid. The equations of

conservation of mass and momentum for such mixtures are formulated for each phase and in the case of intrinsic incompressibility of each constituent, their quasi-static local form can be denoted as:

$$\frac{\partial n^\alpha}{\partial t} + \nabla \cdot (n^\alpha \mathbf{v}^\alpha) = \theta^\alpha, \qquad \alpha = 1, \ldots, \nu \tag{1}$$

$$\nabla \cdot \boldsymbol{\sigma}^\alpha + \boldsymbol{\pi}^\alpha = \mathbf{0}, \qquad \alpha = 1, \ldots, \nu \tag{2}$$

where n^α is the volume fraction, $\mathbf{v}^\alpha$ the velocity, $\boldsymbol{\sigma}^\alpha$ the Cauchy stress tensor and θ^α and $\boldsymbol{\pi}^\alpha$ are the volume and momentum interactions of phase α. The exponent α refers to the constituent number and t is time. Balance of mass for the total mixture requires:

$$\sum_\alpha \theta^\alpha = 0. \tag{3}$$

Likewise for the balance of momentum:

$$\sum_\alpha \boldsymbol{\pi}^\alpha = \mathbf{0}. \tag{4}$$

Furthermore, no moment of momentum interaction between the constituents is assumed, so that $\boldsymbol{\sigma}^\alpha$ is symmetric.

A hierarchical mixture can be thought of to consist of one solid constituent and a fluid constituent that is divided into a continuous series of fluid compartments. Each fluid compartment resides on a specific position in the hierarchy of pores of the solid. The fluid in a compartment flows spatially through the solid (spatial flow) and communicates with compartments on neighbouring hierarchical positions (hierarchical flow). The position in the hierarchy is quantified by a dimensionless parameter x_0, which is assumed to run from zero to one, and the communication between the fluid compartments is described by the fluid volume interaction term θ^f appearing in equation (1). A fluid compartment defined by the hierarchical range $[x_0, x_0 + \mathrm{d}x_0]$ has a volume fraction $\tilde{n}^f \mathrm{d}x_0$ in which $\tilde{n}^f$ represents the fluid volume fraction per unit hierarchical parameter x_0. Generally, in this paper a tilde will be used to indicate that a quantity depends on x_0 and, if the quantity is volume specific, is defined per unit x_0. The exponents s and f refer to solid and fluid, respectively. The mass balance for this fluid compartment is:

$$\frac{\partial \tilde{n}^f}{\partial t}\mathrm{d}x_0 + \nabla \cdot (\tilde{n}^f \tilde{\mathbf{v}}^f)\,\mathrm{d}x_0 = \tilde{n}^f_{(x_0)} \tilde{v}^f_{0(x_0)} - \tilde{n}^f_{(x_0+\mathrm{d}x_0)} \tilde{v}^f_{0(x_0+\mathrm{d}x_0)} \tag{5}$$

in which the right-hand side represents the volume interaction with the neighbouring compartments. $\tilde{v}^f_0$ is a measure of the rate at which fluid flows from one compartment to the next, and is defined as the material time derivative of x_0 with respect to the fluid:

$$\tilde{v}^f_0 = \frac{\mathrm{D}^f x_0}{\mathrm{D}t}. \tag{6}$$

It can be shown that $\tilde{n}^f \tilde{v}^f_0$ corresponds to the traditional, physiological definition of regional blood perfusion [4, 14]. Dividing equation (5) by $\mathrm{d}x_0$ yields for infinitesimal $\mathrm{d}x_0$ the local fluid mass balance:

$$\frac{\partial \tilde{n}^f}{\partial t} + \nabla \cdot (\tilde{n}^f \tilde{\mathbf{v}}^f) = \tilde{\theta}^f = -\frac{\partial (\tilde{n}^f \tilde{v}^f_0)}{\partial x_0}. \tag{7}$$

Assuming no mass interaction between solid and fluid, the mass balance for the total hierarchical mixture (3) can be rewritten as:

$$\theta^s = \int_0^1 \tilde{\theta}^f \,\mathrm{d}x_0 = 0. \tag{8}$$

Because the actual hierarchical fluid volume fraction $\tilde{n}^f$ is defined per unit x_0, saturation of the mixture is expressed as:

$$n^s + \int_0^1 \tilde{n}^f \, dx_0 = n^s + n^f = 1, \tag{9}$$

which can be used in combination with equations (7) and (8) to rewrite solid, fluid and total mass conservation as:

$$-\frac{\partial n^f}{\partial t} + \nabla \cdot ((1 - n^f)\mathbf{v}^s) = 0 \tag{10}$$

$$\frac{\partial \tilde{n}^f}{\partial t} + {}_4\nabla \cdot (\tilde{n}^f \, {}_4\tilde{\mathbf{v}}^f) = 0 \tag{11}$$

$$\nabla \cdot ((1 - n^f)\mathbf{v}^s) + \int_0^1 ({}_4\nabla \cdot (\tilde{n}^f \, {}_4\tilde{\mathbf{v}}^f)) \, dx_0 = 0, \tag{12}$$

where ${}_4\nabla$ is a four-dimensional operator and ${}_4\mathbf{v}^f$ a four-dimensional vector:

$${}_4\nabla = \begin{bmatrix} \dfrac{\partial}{\partial x_0} \\ \nabla \end{bmatrix}, \qquad {}_4\tilde{\mathbf{v}}^f = \begin{bmatrix} \tilde{v}_0^f \\ \tilde{\mathbf{v}}^f \end{bmatrix}. \tag{13}$$

Because the fluid related quantities depend on x_0, the momentum balance of the total hierarchical mixture is written as:

$$\nabla \cdot \boldsymbol{\sigma}^s + \int_0^1 \nabla \cdot \tilde{\boldsymbol{\sigma}}^f \, dx_0 = \mathbf{0} \tag{14}$$

where the balance condition for momentum interaction, equation (4), has been used:

$$\boldsymbol{\pi}^s + \int_0^1 \tilde{\boldsymbol{\pi}}^f \, dx_0 = \mathbf{0}. \tag{15}$$

3. CONSTITUTIVE BEHAVIOUR

In the derivation of requirements for the constitutive behaviour of the hierarchical mixture use is made of the first and second laws of thermodynamics. The first law, conservation of total energy, reads for constituent α of a unit volume of hierarchical mixture [13]:

$$\dot{U}^\alpha = \dot{W}^\alpha + \dot{Q}^\alpha + \dot{E}^\alpha \tag{16}$$

where U^α is the total internal energy, W^α is the external work, Q^α is the heat supply of phase α and E^α is the energy gain of α due to phase interaction. The dots above the variables denote their material time derivatives. Assuming intrinsic incompressibility and quasi-stationarity for each constituent, equation (16) can be written for the solid and fluid constituents in a volume V of hierarchical mixture with surrounding surface A:

$$\text{solid: } \frac{\partial}{\partial t}\left(\int_V n^s U^s \, dV\right) + \int_A n^s U^s \mathbf{v}^s \cdot \mathbf{n} \, dA = \int_A \mathbf{v}^s \cdot \boldsymbol{\sigma}^s \cdot \mathbf{n} \, dA + \int_V n^s r^s \, dV + \int_A \mathbf{h}^s \cdot \mathbf{n} \, dA + \int_V \epsilon^s \, dV + \int_V \boldsymbol{\pi}^s \cdot \mathbf{v}^s \, dV, \tag{17}$$

$$\text{fluid: } \frac{\partial}{\partial t}\left(\int_V \tilde{n}^f \tilde{U}^f \, dV\right) + \int_A \tilde{n}^f \tilde{U}^f \tilde{\mathbf{v}}^f \cdot \mathbf{n} \, dA + \int_V \frac{\partial}{\partial x_0}(\tilde{n}^f \tilde{U}^f \tilde{v}_0^f) \, dV = \int_A \tilde{\mathbf{v}}^f \cdot \tilde{\boldsymbol{\sigma}}^f \cdot \mathbf{n} \, dA + \int_V \frac{\partial}{\partial x_0}(\tilde{v}_0^f \tilde{\sigma}_0^f) \, dV + \int_V \tilde{n}^f \tilde{r}^f \, dV + \int_A \tilde{\mathbf{h}}^f \cdot \mathbf{n} \, dA + \int_V \frac{\partial}{\partial x_0}(\tilde{h}_0^f) \, dV + \int_V \tilde{\epsilon}^f \, dV + \int_V \tilde{\boldsymbol{\pi}}^f \cdot \tilde{\mathbf{v}}^f \, dV, \tag{18}$$

where r^α is the internal heat supply, $\mathbf{h}^\alpha$ the external heat supply and ϵ^α the direct energy supply of constituent α due to phase interaction. $\tilde{\sigma}_0^{\mathrm{f}}$ is the fluid stress at the interface between neighbouring hierarchical levels and h_0^{f} the heat supply between neighbouring hierarchical levels. Note that equation (18) is expressed per unit of x_0, and that internal energy variation of the fluid due to volume interaction is included in the third term. Applying Gauss' theorem gives for the local conservation of total energy of the solid and the fluid:

$$\text{solid: } \frac{\partial}{\partial t}(n^{\mathrm{s}}U^{\mathrm{s}}) = -\nabla\cdot(n^{\mathrm{s}}U^{\mathrm{s}}\mathbf{v}^{\mathrm{s}}) + \nabla\cdot(\mathbf{v}^{\mathrm{s}}\cdot\boldsymbol{\sigma}^{\mathrm{s}}) + n^{\mathrm{s}}r^{\mathrm{s}} + \nabla\cdot\mathbf{h}^{\mathrm{s}} + \epsilon^{\mathrm{s}} + (\boldsymbol{\pi}^{\mathrm{s}}\cdot\mathbf{v}^{\mathrm{s}}), \tag{19}$$

$$\text{fluid: } \frac{\partial}{\partial t}(\tilde{n}^{\mathrm{f}}\tilde{U}^{\mathrm{f}}) = -\nabla\cdot(\tilde{n}^{\mathrm{f}}\tilde{U}^{\mathrm{f}}\tilde{\mathbf{v}}^{\mathrm{f}}) - \frac{\partial}{\partial x_0}(\tilde{n}^{\mathrm{f}}\tilde{U}^{\mathrm{f}}\tilde{v}_0^{\mathrm{f}}) + \nabla\cdot(\tilde{\mathbf{v}}^{\mathrm{f}}\cdot\tilde{\boldsymbol{\sigma}}^{\mathrm{f}}) + \frac{\partial}{\partial x_0}(\tilde{v}_0^{\mathrm{f}}\tilde{\sigma}_0^{\mathrm{f}})$$

$$+ \tilde{n}^{\mathrm{f}}\tilde{r}^{\mathrm{f}} + \nabla\cdot\tilde{\mathbf{h}}^{\mathrm{f}} + \frac{\partial}{\partial x_0}(\tilde{h}_0^{\mathrm{f}}) + \tilde{\epsilon}^{\mathrm{f}} + \tilde{\boldsymbol{\pi}}^{\mathrm{f}}\cdot\tilde{\mathbf{v}}^{\mathrm{f}}, \tag{20}$$

which can be rewritten by using the material time derivative of U, and the local mass and momentum balances equations (10) and (11):

$$\text{solid: } n^{\mathrm{s}}\frac{\mathrm{D}^{\mathrm{s}}U^{\mathrm{s}}}{\mathrm{D}t} = \boldsymbol{\sigma}^{\mathrm{s}}:(\nabla\mathbf{v}^{\mathrm{s}}) + n^{\mathrm{s}}r^{\mathrm{s}} + \nabla\cdot\mathbf{h}^{\mathrm{s}} + \epsilon^{\mathrm{s}}, \tag{21}$$

$$\text{fluid: } \tilde{n}^{\mathrm{f}}\frac{\mathrm{D}^{\mathrm{f}}\tilde{U}^{\mathrm{f}}}{\mathrm{D}t} = \tilde{\boldsymbol{\sigma}}^{\mathrm{f}}:(\nabla\tilde{\mathbf{v}}^{\mathrm{f}}) + \frac{\partial}{\partial x_0}(\tilde{\sigma}_0^{\mathrm{f}}\tilde{v}_0^{\mathrm{f}}) + \tilde{n}^{\mathrm{f}}\tilde{r}^{\mathrm{f}} + {}_4\nabla\cdot{}_4\tilde{\mathbf{h}}^{\mathrm{f}} + \tilde{\epsilon}^{\mathrm{f}}. \tag{22}$$

In equation (22) use has also been made of the four-dimensional gradient operator ${}_4\nabla$ and fluid velocity ${}_4\tilde{\mathbf{v}}^{\mathrm{f}}$ [equation (13)] and the analogously defined external heat supply ${}_4\tilde{\mathbf{h}}^{\mathrm{f}}$:

$${}_4\tilde{\mathbf{h}}^{\mathrm{f}} = \begin{bmatrix}\tilde{h}_0^{\mathrm{f}}\\ \tilde{\mathbf{h}}^{\mathrm{f}}\end{bmatrix}. \tag{23}$$

The local balance condition of the energy interaction of the total mixture requires that no energy is created by the interaction:

$$\epsilon^{\mathrm{s}} + \boldsymbol{\pi}^{\mathrm{s}}\cdot\mathbf{v}^{\mathrm{s}} + \int_0^1(\tilde{\epsilon}^{\mathrm{f}} + \tilde{\boldsymbol{\pi}}^{\mathrm{f}}\cdot\tilde{\mathbf{v}}^{\mathrm{f}})\,\mathrm{d}x_0 = 0. \tag{24}$$

At this point the second law of thermodynamics, the entropy inequality, is introduced:

$$\mathrm{d}S \geq \frac{\mathrm{d}Q}{T} \tag{25}$$

which relates the change of entropy of the total hierarchical mixture, $\mathrm{d}S$, to the supplied heat $\mathrm{d}Q$ at a temperature T. For a volume V of mixture with surrounding surface A and constant temperature T in each constituent this can be written as:

$$\frac{\partial}{\partial t}\left(\int_V n^{\mathrm{s}}S^{\mathrm{s}}\,\mathrm{d}V\right) + \int_A n^{\mathrm{s}}S^{\mathrm{s}}\mathbf{v}^{\mathrm{s}}\cdot\mathbf{n}\,\mathrm{d}A$$

$$+ \int_0^1\left[\frac{\partial}{\partial t}\left(\int_V \tilde{n}^{\mathrm{f}}\tilde{S}^{\mathrm{f}}\,\mathrm{d}V\right) + \int_A \tilde{n}^{\mathrm{f}}\tilde{S}^{\mathrm{f}}\tilde{\mathbf{v}}^{\mathrm{f}}\cdot\mathbf{n}\,\mathrm{d}A + \int_V\frac{\partial}{\partial x_0}(\tilde{n}^{\mathrm{f}}\tilde{S}^{\mathrm{f}}\tilde{v}_0^{\mathrm{f}})\,\mathrm{d}V\right]\mathrm{d}x_0$$

$$\geq \int_V\frac{n^{\mathrm{s}}r^{\mathrm{s}}}{T}\,\mathrm{d}V + \int_A\frac{\mathbf{h}^{\mathrm{s}}\cdot\mathbf{n}}{T}\,\mathrm{d}A + \int_0^1\left[\int_V\frac{\tilde{n}^{\mathrm{f}}\tilde{r}^{\mathrm{f}}}{T}\,\mathrm{d}V + \int_A\frac{\tilde{\mathbf{h}}^{\mathrm{f}}\cdot\mathbf{n}}{T}\,\mathrm{d}A + \int_V\frac{\partial}{\partial x_0}\left(\frac{\tilde{h}_0^{\mathrm{f}}}{T}\right)\mathrm{d}V\right]\mathrm{d}x_0. \tag{26}$$

By applying Gauss' theorem and making use of the material time derivative of S, the local form of equation (26) can be written as:

$$n^s \frac{D^s S^s}{Dt} + \int_0^1 \left(\tilde{n}^f \frac{D^f \tilde{S}^f}{Dt} \right) dx_0 \geq \frac{1}{T} \left(n^s r^s + \nabla \cdot \mathbf{h}^s + \int_0^1 (\tilde{n}^f \tilde{r}^f + {}_4\nabla \cdot {}_4\tilde{\mathbf{h}}^f)\, dx_0 \right). \tag{27}$$

Substituting the local energy equations for solid and fluid, equations (21) and (22), into the local entropy inequality, equation (27), yields:

$$n^s \frac{D^s S^s}{Dt} + \int_0^1 \left(\tilde{n}^f \frac{D^f \tilde{S}^f}{Dt} \right) dx_0$$
$$\geq \frac{1}{T} \left(n^s \frac{D^s U^s}{Dt} - \boldsymbol{\sigma}^s : (\nabla \mathbf{v}^s) + \boldsymbol{\pi}^s \cdot \mathbf{v}^s + \int_0^1 \left[\tilde{n}^f \frac{D^f \tilde{U}^f}{Dt} - \tilde{\boldsymbol{\sigma}}^f : (\nabla \tilde{\mathbf{v}}^f) - \frac{\partial}{\partial x_0} (\tilde{\sigma}_0^f \tilde{v}_0^f) + \tilde{\boldsymbol{\pi}}^f \cdot \tilde{\mathbf{v}}^f \right] dx_0 \right) \tag{28}$$

in which the total energy interaction $\epsilon^s + \int_0^1 \tilde{\epsilon}^f dx_0$ was eliminated by means of equation (24). Introducing Helmholtz' free energy $F = U - TS$ for each constituent, and substituting momentum balance equation (14) yields:

$$\frac{1}{T} \left(-n^s \frac{D^s F^s}{Dt} + \boldsymbol{\sigma}^s : (\nabla \mathbf{v}^s) + \mathbf{v}^s \cdot (\nabla \cdot \boldsymbol{\sigma}^s) \right.$$
$$\left. + \int_0^1 \left[-\tilde{n}^f \frac{D^f \tilde{F}^f}{Dt} + \tilde{\boldsymbol{\sigma}}^f : (\nabla \tilde{\mathbf{v}}^f) + \tilde{\mathbf{v}}^f \cdot (\nabla \cdot \tilde{\boldsymbol{\sigma}}^f) + \frac{\partial}{\partial x_0} (\tilde{\sigma}_0^f \tilde{v}_0^f) \right] dx_0 \right) \geq 0. \tag{29}$$

Expressing equation (29) per unit of undeformed volume of mixture and transforming the material time derivative of F^f yields:

$$-Jn^s \frac{D^s F^s}{Dt} + J\, \nabla \cdot (\boldsymbol{\sigma}^s \cdot \mathbf{v}^s) + \int_0^1 \left[-J\tilde{n}^f \frac{D^s \tilde{F}^f}{Dt} + J_4 \nabla \cdot ({}_4\tilde{\boldsymbol{\sigma}}^f \cdot {}_4\tilde{\mathbf{v}}^f) - J\tilde{n}^f ({}_4\tilde{\mathbf{v}}^f - {}_4\mathbf{v}^s) \cdot {}_4\tilde{\nabla} \tilde{F} \right] dx_0 \geq 0. \tag{30}$$

For compactness of notation, the four-dimensional fluid stress tensor ${}_4\tilde{\boldsymbol{\sigma}}^f$ and solid velocity vector ${}_4\mathbf{v}^s$ have been used, which can be written in matrix notation as:

$${}_4\tilde{\boldsymbol{\sigma}}^f = \begin{bmatrix} \tilde{\sigma}_0^f & \mathbf{0} \\ \mathbf{0} & \tilde{\boldsymbol{\sigma}}^f \end{bmatrix}; \qquad {}_4\mathbf{v}^s = \begin{bmatrix} 0 \\ \mathbf{v}^s \end{bmatrix}. \tag{31}$$

Again rewriting the material time derivatives of F gives:

$$-\frac{D^s J n^s F^s}{Dt} + F^s \frac{D^s J n^s}{Dt} + J\, \nabla \cdot (\boldsymbol{\sigma}^s \cdot \mathbf{v}^s)$$
$$+ \int_0^1 \left[-\frac{D^s J\tilde{n}^f \tilde{F}^f}{Dt} + \tilde{F}^f \frac{D^s J\tilde{n}^f}{Dt} - J\tilde{n}^f ({}_4\tilde{\mathbf{v}}^f - {}_4\mathbf{v}^s) \cdot {}_4\nabla \tilde{F}^f + J_4 \nabla \cdot ({}_4\tilde{\boldsymbol{\sigma}}^f \cdot {}_4\tilde{\mathbf{v}}^f) \right] dx_0 \geq 0. \tag{32}$$

Because of incompressibility of the solid, $D^s(Jn^s)/Dt = 0$. Substituting the Lagrangian form of the equation of conservation of fluid mass [equation (11)]

$$\frac{D^s (J\tilde{n}^f)}{Dt} + J_4 \nabla \cdot (\tilde{n}^f ({}_4\tilde{\mathbf{v}}^f - {}_4\mathbf{v}^s)) = 0 \tag{33}$$

in equation (32) yields:

$$\int_0^1 \left[-\frac{D^s \tilde{W}}{Dt} + J\, \nabla \cdot (\boldsymbol{\sigma}^s \cdot \mathbf{v}^s) - \tilde{F}^f J_4 \nabla (\tilde{n}^f ({}_4\tilde{\mathbf{v}}^f - {}_4\mathbf{v}^s)) - J\tilde{n}^f ({}_4\tilde{\mathbf{v}}^f - {}_4\mathbf{v}^s) \cdot {}_4\nabla \tilde{F}^f + J_4 \nabla \cdot ({}_4\tilde{\boldsymbol{\sigma}}^f \cdot {}_4\tilde{\mathbf{v}}^f) \right] dx_0 \geq 0, \tag{34}$$

where the strain energy function $\tilde{W} = Jn^s F^s + J\tilde{n}^f \tilde{F}^f$ has been introduced. By using the total stress defined as $\boldsymbol{\sigma} = \boldsymbol{\sigma}^s + \int_0^1 \tilde{\boldsymbol{\sigma}}^f \, dx_0$, equation (34) can be written as:

$$J\boldsymbol{\sigma} : (\nabla \mathbf{v}^s) + \int_0^1 \left[-\frac{D^s \tilde{W}}{Dt} - J\, {}_4\nabla \cdot (\tilde{n}^f ({}_4\tilde{\mathbf{v}}^f - {}_4\mathbf{v}^s)\tilde{F}^f) + J\nabla \cdot (({}_4\tilde{\mathbf{v}}^f - {}_4\mathbf{v}^s) \cdot {}_4\tilde{\boldsymbol{\sigma}}^f) \right] dx_0 \geq 0. \tag{35}$$

Expressing the free energy of the fluid per unit mixture volume as $\tilde{\psi}^f = \tilde{n}^f \tilde{F}^f$, introducing the well-known effective stress $\boldsymbol{\sigma}^{eff} = \boldsymbol{\sigma} + p\mathbf{I}$ [15] and adding the total mass balance equation (12) with a Lagrange multiplier p, equation (35) can be written as:

$$J\boldsymbol{\sigma}^{eff} : (\nabla \mathbf{v}^s) + \int_0^1 \left[-\frac{D^s \tilde{W}}{Dt} + J({}_4\tilde{\boldsymbol{\sigma}}^f - \tilde{\psi}^f {}_4\mathbf{I} - p\tilde{n}^f {}_4\mathbf{I}) : {}_4\nabla({}_4\tilde{\mathbf{v}}^f - {}_4\mathbf{v}^s) \right.$$

$$\left. + J({}_4\tilde{\mathbf{v}}^f - {}_4\mathbf{v}^s) \cdot ({}_4\nabla \cdot {}_4\tilde{\boldsymbol{\sigma}}^f - {}_4\nabla\tilde{\psi}^f + p\, {}_4\nabla\tilde{n}^f) \right] dx_0 \geq 0 \tag{36}$$

where ${}_4\mathbf{I}$ represents the four-dimensional unity tensor. We choose as independent variables the Green–Lagrange strain tensor $\mathbf{E}$, the Lagrangian form of the fluid volume fraction $J\tilde{n}^f$ and the relative velocity ${}_4\tilde{\mathbf{v}}^{fs} = {}_4\mathbf{F}^{-1} \cdot ({}_4\tilde{\mathbf{v}}^f - {}_4\mathbf{v}^s)$. For convenience of notation we introduced the four-dimensional tensor ${}_4\mathbf{F}$:

$${}_4\mathbf{F} = \begin{bmatrix} 1 & \mathbf{0} \\ \mathbf{0} & \mathbf{F} \end{bmatrix}, \tag{37}$$

in which $\mathbf{F}$ is the deformation tensor. Applying the principle of equipresence and the chain rule for time differentiation of $\tilde{W}$ and defining $W = \int_0^1 \tilde{W} \, dx_0$, yields the inequality:

$$\left[J\boldsymbol{\sigma}^{eff} - \mathbf{F} \cdot \frac{\partial W}{\partial \mathbf{E}} \cdot \mathbf{F}^c \right] : \nabla \mathbf{v}^s + \int_0^1 \left[-\frac{\partial \tilde{W}}{\partial\, {}_4\tilde{\mathbf{v}}^{fs}} \cdot \frac{D^s\, {}_4\tilde{\mathbf{v}}^{fs}}{Dt} + J({}_4\tilde{\boldsymbol{\sigma}}^f + (\tilde{\mu}^f \tilde{n}^f - \tilde{\psi}^f) {}_4\mathbf{I}) : {}_4\nabla({}_4\tilde{\mathbf{v}}^f - {}_4\mathbf{v}^s) \right.$$

$$\left. + J({}_4\tilde{\mathbf{v}}^f - {}_4\mathbf{v}^s) \cdot (-{}_4\nabla\tilde{\psi}^f + \tilde{\mu}^f\, {}_4\nabla\tilde{n}^f + {}_4\nabla \cdot {}_4\tilde{\boldsymbol{\sigma}}^f) \right] dx_0 \geq 0 \tag{38}$$

which should be true for any value of the state variables. Here use has been made of the definition of the chemical potential of the fluid:

$$\tilde{\mu}^f = \frac{\partial \tilde{W}}{\partial (J\tilde{n}^f)} + p. \tag{39}$$

The fourth term of the left-hand side of equation (38) represents the dissipation due to fluid flow. The first term is linear in the solid velocity gradient, the second linear in the accelerations and the third linear in the relative velocity gradients. Therefore, by a standard argument, we find the constitutive relations:

$$\boldsymbol{\sigma}^{eff} = \frac{1}{J} \mathbf{F} \cdot \frac{\partial W}{\partial \mathbf{E}} \cdot \mathbf{F}^c \tag{40}$$

$$\frac{\partial \tilde{W}}{\partial\, {}_4\tilde{\mathbf{v}}^{fs}} = {}_4\mathbf{0} \tag{41}$$

$${}_4\tilde{\boldsymbol{\sigma}}^f = (\tilde{\psi}^f - \tilde{\mu}^f \tilde{n}^f) {}_4\mathbf{I} \tag{42}$$

leaving as inequality:

$$J \int_0^1 [({}_4\tilde{\mathbf{v}}^f - {}_4\mathbf{v}^s) \cdot (-{}_4\nabla\tilde{\psi}^f + \tilde{\mu}^f\, {}_4\nabla\tilde{n}^f + {}_4\nabla \cdot {}_4\tilde{\boldsymbol{\sigma}}^f)] \, dx_0 \geq 0. \tag{43}$$

If we assume that dissipation associated with fluid flow is a quadratic function of the fluid velocities we find:

$$-{}_4\nabla_0\tilde{\psi}^{\mathrm{f}} + \tilde{\mu}^{\mathrm{f}}\,{}_4\nabla_0\tilde{n}^{\mathrm{f}} + {}_4\nabla_0 \cdot {}_4\tilde{\boldsymbol{\sigma}}^{\mathrm{f}} = {}_4\tilde{\mathbf{B}}^{\mathrm{f}} \cdot {}_4\tilde{\mathbf{v}}^{\mathrm{fs}}. \tag{44}$$

Substituting the constitutive expression equation (42) of the fluid stress ${}_4\tilde{\boldsymbol{\sigma}}^{\mathrm{f}}$ into equation (44), yields the extended Darcy equation:

$$-\tilde{n}^{\mathrm{f}}\,{}_4\nabla_0\tilde{\mu}^{\mathrm{f}} = {}_4\tilde{\mathbf{B}}^{\mathrm{f}} \cdot {}_4\tilde{\mathbf{v}}^{\mathrm{fs}} \tag{45}$$

which can be written in a more common form [4]:

$$\tilde{n}^{\mathrm{f}}\,{}_4\tilde{\mathbf{v}}^{\mathrm{fs}} = -{}_4\tilde{\mathbf{K}} \cdot {}_4\nabla_0\tilde{\mu}^{\mathrm{f}} \tag{46}$$

in which the four-dimensional permeability tensor ${}_4\tilde{\mathbf{K}}$ reads:

$${}_4\tilde{\mathbf{K}} = (\tilde{n}^{\mathrm{f}})^2\,{}_4\tilde{\mathbf{B}}^{\mathrm{f}^{-1}} = \begin{bmatrix} \tilde{k}_{00} & \tilde{\mathbf{k}}_0 \\ \tilde{\mathbf{k}}_0 & \tilde{\mathbf{K}} \end{bmatrix}. \tag{47}$$

4. NUMERICAL IMPLEMENTATION

The hierarchical mixture model has been implemented in the finite element software package DIANA. The displacement of the solid $\mathbf{u}^{\mathrm{s}}$, the hydrostatic pressure p and the fluid pressure $\tilde{\mu}^{\mathrm{f}}$ have been chosen as the degrees of freedom. Three equations are used (i) the momentum balance (2), in which the constitutive equation for the effective stress (40) is substituted; (ii) the solid mass balance (10); and (iii) the fluid mass balance (11), in which the extended Darcy equation (46) is substituted. The weighted residual method has been applied to the resulting system of non-linear coupled differential equations. After spatial discretization of the degrees of freedom the weighting functions are chosen according to Galerkin's method. Special attention was paid to the discretization of the fluid pressure $\tilde{\mu}^{\mathrm{f}}$, which depends on both spatial position $\mathbf{x}$ and x_0. Its spatial discretization was achieved analogously to the hydrostatic pressure's discretization, while an extra linear discretization in the x_0 direction was used. A more detailed description of the finite element formulation and implementation is given in [16]. The resulting total element matrix equation is:

$$\begin{bmatrix} 0 & 0 & 0 \\ {}^{\mathrm{u}}_{\mathrm{s}}B^{IL}_{j} & {}^{\mathrm{p}}_{\mathrm{s}}B^{JM} & {}^{\mu^{\mathrm{f}}}_{\mathrm{s}}B^{JN}_{n} \\ 0 & {}^{\mathrm{p}}_{\mathrm{f}}B^{KM}_{k} & {}^{\mu^{\mathrm{f}}}_{\mathrm{f}}B^{KN}_{kn} \end{bmatrix} \begin{bmatrix} \delta\dot{u}^{L}_{j} \\ \delta\dot{p}^{M} \\ \delta\dot{\tilde{\mu}}^{\mathrm{f}^{N}}_{n} \end{bmatrix} + \begin{bmatrix} {}^{\mathrm{u}}_{\mathrm{m}}K^{IL}_{ij} & {}^{\mathrm{p}}_{\mathrm{m}}K^{IM}_{i} & 0 \\ 0 & 0 & 0 \\ 0 & 0 & {}^{\mu^{\mathrm{f}}}_{\mathrm{f}}K^{KN}_{kn} \end{bmatrix} \begin{bmatrix} \delta u^{L}_{j} \\ \delta p^{M} \\ \delta\tilde{\mu}^{\mathrm{f}^{N}}_{n} \end{bmatrix} = \begin{bmatrix} {}_{\mathrm{m}}R^{I}_{\mathrm{ex}i} \\ 0 \\ {}_{\mathrm{f}}R^{K}_{\mathrm{ex}k} \end{bmatrix} - \begin{bmatrix} {}_{\mathrm{m}}R^{I}_{\mathrm{in}i} \\ {}_{\mathrm{s}}R^{J}_{\mathrm{in}} \\ {}_{\mathrm{f}}R^{K}_{\mathrm{in}k} \end{bmatrix} \tag{48}$$

where δu^{L}_{j} is the iterative correction of displacement component in direction j of node L, δp^{M} is the iterative correction of hydrostatic pressure in node M, $\delta\tilde{\mu}^{\mathrm{f}^{N}}_{n}$ is the iterative correction of fluid pressure at hierarchical level n is node N, and a dot above a variable denotes its material time derivative. In this matrix equation symmetry is found in the submatrices ${}^{\mathrm{p}}_{\mathrm{s}}\mathbf{B}$, ${}^{\mu^{\mathrm{f}}}_{\mathrm{f}}\mathbf{B}$, ${}^{\mathrm{u}}_{\mathrm{m}}\mathbf{K}$, ${}^{\mu^{\mathrm{f}}}_{\mathrm{f}}\mathbf{K}$ and moreover ${}^{\mathrm{p}}_{\mathrm{f}}B^{KM}_{k} = {}^{\mu^{\mathrm{f}}}_{\mathrm{s}}B^{MK}_{k}$ and ${}^{\mathrm{u}}_{\mathrm{s}}B^{IL}_{j} = {}^{\mathrm{p}}_{\mathrm{m}}K^{LJ}_{j}$. Thus a fully symmetric matrix equation can be obtained after time integration of the damping contribution. This time integration is achieved by a third-order Houbolt scheme [17]:

$$\dot{s}(t) = h_0 s(t) + \sum_{i=1}^{3} h_i s(t - \tau_i); \qquad s = \mathbf{u}^{\mathrm{s}}, p, \tilde{\mu}^{\mathrm{f}}. \tag{49}$$

Linear and quadratic two-dimensional, axi-symmetric and three-dimensional isoparametric elements of the serendipity family can be used [18]. The non-linear equations can be solved by several regular and modified Newton–Raphson iteration techniques and a direct Gauss decomposition [19]. The implementation has been tested for several problems. Rigid body

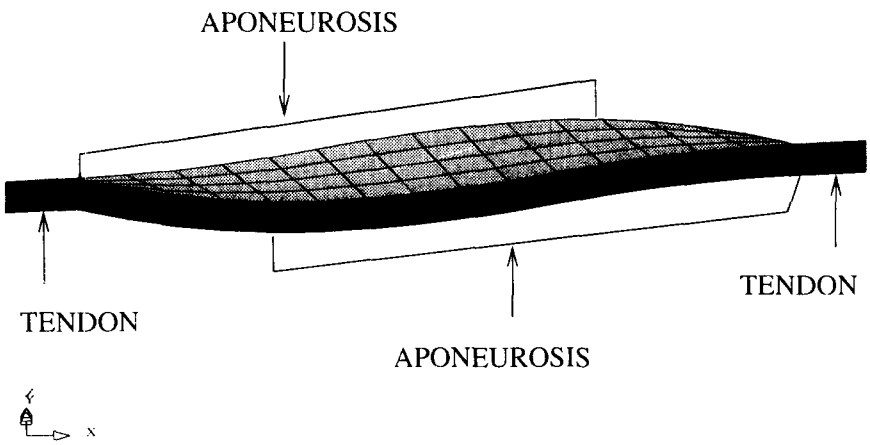

Fig. 2. Finite element model geometry. The mesh consists of 112 six-node wedge-shaped three-dimensional elements for the muscle belly, 22 three-node triangular plane stress elements for each aponeurosis and two three-node triangular plane stress elements for each tendon.

rotations and translations and analytical solutions of a one-dimensional confined compression experiment and a four-dimensional Laplace equation have been successfully computed [16].

5. APPLICATION

A simulation of a perfusion experiment on an isometrically (at constant length) and tetanically (sustained) contracting skeletal muscle has been performed, using the finite element model. The muscle under consideration is a rat calf muscle (*gastrocnemius medialis*), of which the geometry has been roughly estimated from experimental measurements. This muscle is about 30 mm long and 6 mm thick. The model geometry and mesh are given in Fig. 2. The tendons and aponeuroses (tendinous sheets on the muscle surface by which the tendons are attached to the muscle belly) are marked by the dark regions in Fig. 2. The tendons, each consisting of two triangular three-node plane stress elements, and the aponeuroses, each consisting of 22 similar elements, behave isotropically and linearly elastically with a Young's modulus of 1.5×10^6 kPa [20] and Poisson's ratio of 0.3. The thickness of the tendons is 0.5 mm. The thickness of the aponeuroses runs from 0.5 mm at the tendon to 0.01 mm at the other end.

The passive material behaviour of the muscle tissue is based on a transverse isotropic, non-linearly elastic description of cardiac tissue according to Bovendeerd [21]. The direction of anisotropy (e_1) corresponds with the direction of the muscle fibres (Fig. 2), and the contribution of the local Green strain in the tissue to the elastic energy is:

$$W_E = C[e^{a(2E_{11}^2+E_{22}^2+E_{33}^2+2E_{12}^2+2E_{23}^2+2E_{31}^2)} - 1] \tag{50}$$

where $C = 0.7$ kPa and $a = 5.0$. The elastic energy is assumed to depend also on strain in the vessel walls, which is associated with changes in vascular volume. The contribution of the vessel strain to the elastic energy is expressed as:

$$W_C = \frac{1}{2\tilde{c}}(J\tilde{n}^f)^2 \tag{51}$$

where the vessel compliance $\tilde{c}$ represents the relation between the local blood volume fraction and local intra–extra vascular pressure difference:

$$\tilde{c} = \frac{\partial(J\tilde{n}^f)}{\partial(\tilde{\mu}^f - p)}. \tag{52}$$

Table 1. Vascular parameters

	$\tilde{K}\left(\frac{\text{mm}^2}{\text{s kPa}}\right)$	$\tilde{k}_{00}\left(\frac{1}{\text{s kPa}}\right)$	$\tilde{c}\left(\frac{1}{\text{kPa}}\right)$
Arterial	100	0.0025	0.001
Arteriolar	0.05	0.00025	0.01
Venular	0.02	0.0025	0.1

The values for $\tilde{c}$ that were used in the simulation are listed in Table 1. Thus the total strain energy function of the muscle material reads:

$$W = W_E + W_C = C[e^{a(2E_{11}^2+E_{22}^2+E_{33}^2+2E_{12}^2+2E_{23}^2+2E_{31}^2)} - 1] + \frac{1}{2\tilde{c}}(J\tilde{n}^f)^2. \tag{53}$$

Contraction is described as an active second Piola–Kirchhoff stress component in fibre direction depending on time:

$$s_f = \frac{S_{max}}{\lambda_f}\left(1 - \left(\frac{1}{(1+(t/t_r)^4)}\right)\right) \tag{54}$$

where $S_{max} = 100$ kPa, λ_f is the relative elongation in the direction, $t_r = 0.05$ s, and t is time (s). This contraction function is a rough approximation of the stress generation in tetanic contraction of rat *gastrocnemius medialis* muscle as described by Huijing and Rozendal [22].

Discretization of the hierarchical range is achieved by three linear segments, resulting in arterial, arteriolar, capillary and venous blood pressures in each spatial nodal point. The vascular segments are assumed to represent the arterial bed, arteriolar bed and the capillary–venous bed, respectively (Fig. 3). The permeability tensor ${}_4\tilde{\mathbf{K}}$ and the vessel compliance $\tilde{c}$ are prescribed for each compartment according to Table 1, whereas they are constant in the whole geometry. For the sake of simplicity ${}_4\tilde{\mathbf{K}}$, which is defined according to equation (47), is assumed to be diagonal, where $\tilde{\mathbf{K}} = \tilde{K}\mathbf{I}$.

We assume that the main artery and vein penetrate into the muscle at the tip of one of the aponeuroses (Fig. 2). At that position the nodal arterial input pressure is set at 10 kPa, and nodal venous outflow pressure at 0 kPa. No force load is applied to the muscle. Due to these

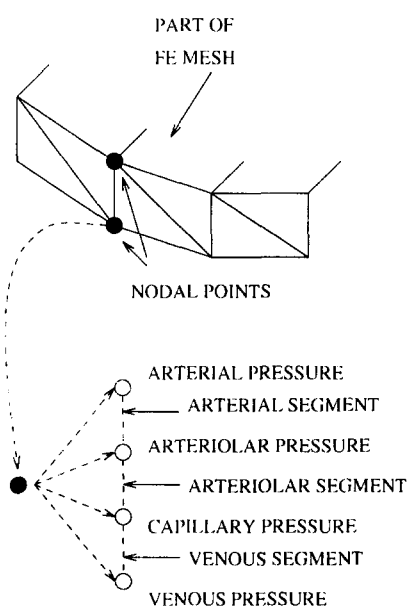

Fig. 3. Illustration of the division of the fluid into three segments, from which four blood pressures result in each nodal point.

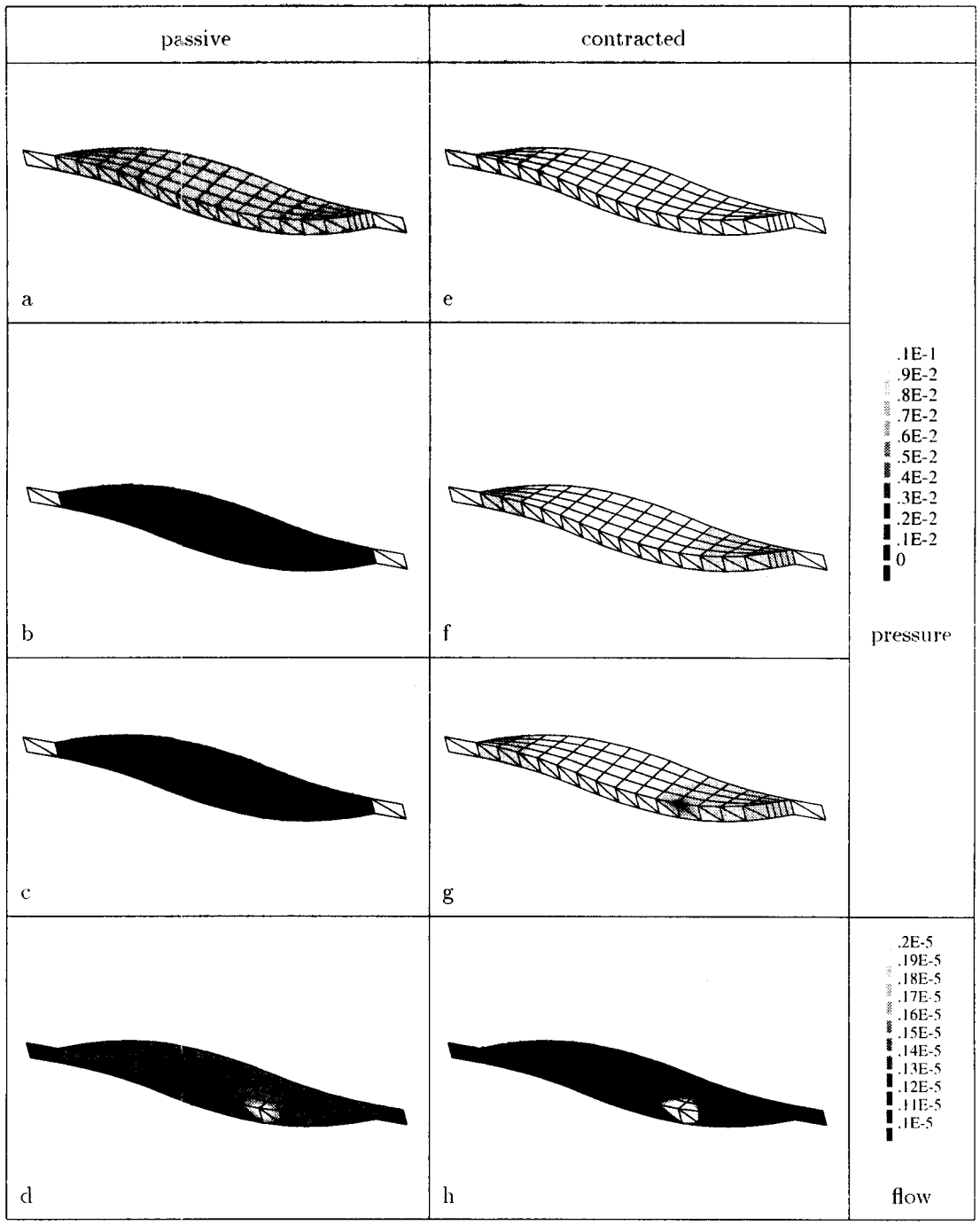

Fig. 4. Contours of blood pressures (MPa) and hierarchical flows (1/ms) in passive and contracting muscle. (a) Passive arterial blood pressure; (b) passive capillary blood pressure; (c) passive venous blood pressure; (d) passive hierarchic capillary flow; (e) arterial blood pressure during contraction; (f) capillary blood pressure during contraction; (g) venous blood pressure during contraction; (h) hierarchic capillary flow during contraction.

nodal boundary conditions a stationary blood flow pattern is reached after about 0.3 s. In Fig. 4(a–c) contours of arterial, capillary and venous blood pressures are given. Also, hierarchic capillary flow (volume averaged blood flow through the capillary compartment, which corresponds to the physiological definition of regional capillary perfusion, defined as volume of blood passing the capillaries per second and per volume of tissue) is given in Fig. 4(d). The

calculated values approximate experimentally measured values, which were found to be about $2.5 \times 10^{-3}\,s^{-1}$ in resting skeletal muscle [23].

When the muscle is in the stationary perfusion state, contraction is started. After 0.1 s the contraction stress has reached its maximum value. Due to the contraction, a significant rise in interstitial pressure (hydrostatic pressure in the solid) occurs, which is transmitted to the blood via the elastic vessel walls. The arterial blood pressure increases slightly [Fig. 4(e)]. Capillary and venous pressure, however, increase drastically [Figs 4(f, g)]. Moreover, we find a strongly decreased hierarchical flow for the capillary blood [Fig. 4(h)], which is due to the decreased pressure difference between the capillary and venous compartments.

6. DISCUSSION

In this paper, mixture theory has been applied to finite deformation of incompressible elastic porous media saturated with a series of intercommunicating fluid compartments. The resulting equations are moulded into a family of finite elements. The finite element model is applied to a simulation of blood perfusion of contracting skeletal muscle. Among others, the model predicts regional hierarchical flow, a quantity that corresponds to the physiologically relevant quantity of regional capillary blood perfusion.

Finite element analysis often aims at predicting failure of structures. Whereas failure of technical materials is mostly associated with excess stress, biological material often fails due to disturbance of the supply of nutrients and drainage of waste matter. Finite element analysis of technical structures therefore focuses on stress analysis, whereas finite element analysis of biological structures ought to pursue a broader scope of mechanical function, including remodelling processes and transport phenomena. We believe it is essential to include regional capillary blood perfusion, being a key quantity for transport through many biological tissues, as a field variable in the analysis of mechanical function of biological tissues. Moreover, tissue deformation and blood perfusion are mechanically linked [24, 25]. The model presented in this paper specifically describes the mechanical interaction between blood perfusion and deformation of the tissue, and as such may provide a better insight into this interaction.

In the simulation it is shown that in an isometrically contracting skeletal muscle, the rise in interstitial pressure is transferred particularly to the capillary and venous blood compartments, which results in a decrease of the capillary hierarchical flow (regional capillary perfusion), which is consistent with experiments reported in [26].

The permeability tensor ${}_4\tilde{\mathbf{K}}$ contains much information about vessel distribution, vessel directions and vessel density for each compartment and each mesh element. As no values for ${}_4\tilde{\mathbf{K}}$ were available, it was made diagonal for the sake of simplicity. However, values for ${}_4\tilde{\mathbf{K}}$ can be derived from geometrical information of a vascular tree [4, 5]. This information can, for example, be obtained by reconstruction of the vasculature by corrosion casting. For the large arterial and venous vessels, the vessel density of the tissue is very low and inhomogeneous which makes them relatively easy to reconstruct. Accurate simulation of the perfusion in these compartments, however, might need special attention, because the model deals with volume averaged quantities, which intrinsically assume homogeneity within the averaging volume. On the other hand, the small vessels like arterioles and capillaries, which are tedious to reconstruct because of their huge density, can be described rather well by the volume averaged relations of the model.

REFERENCES

[1] C. W. J. OOMENS, D. H. VAN CAMPEN and H. J. GROOTENBOER, *J. Biomechanics* **20,** 877 (1987).
[2] W. M. LAI, J. S. HOU and V. C. MOW, *J. Biomech. Engng* **113,** 245 (1991).
[3] J. M. HUYGHE, T. ARTS, D. H. VAN CAMPEN and R. S. RENEMAN, *Am. J. Physiol.* **262,** H1256 (1992).

[4] J. M. HUYGHE, C. W. OOMENS, D. H. VAN CAMPEN and R. M. HEETHAAR, *Biorheology* **26,** 55 (1989).
[5] J. M. HUYGHE, C. W. OOMENS and D. H. VAN CAMPEN, *Biorheology* **26,** 73 (1989).
[6] J. I. E. HOFFMAN and J. A. E. SPAAN, *Physiol. Rev.* **70,** 331 (1990).
[7] E. C. AIFANTIS, *Dev. Mech.* **8,** 209 (1977).
[8] R. K. WILSON and E. C. AIFANTIS, *Int. J. Engng Sci.* **20,** 1009 (1982).
[9] J. M. HUYGHE and D. H. VAN CAMPEN, *Int. J. Engng Sci.* **33,** 1861 (1995).
[10] J. M. HUYGHE and D. H. VAN CAMPEN, *Int. J. Engng Sci.* **33,** 1873 (1995).
[11] R. DE BORST, G. M. A. KUSTERS, P. NAUTA and F. C. DE WITTE, *Finite Element Systems: A Handbook* (Edited by C. A. BREBBIA). Springer, Berlin (1985).
[12] A. BEDFORD and D. S. DRUMHELLER, *Int. J. Engng Sci.* **21,** 863 (1983).
[13] R. M. BOWEN, *Int. J. Engng Sci.* **18,** 1129 (1980).
[14] A. C. GUYTON, *Textbook of Medical Physiology*, 7th edn. W. B. Saunders, Philadelphia (1986).
[15] K. TERZAGHI, *Theoretical Soil Mechanics*. John Wiley, New York (1943).
[16] W. J. VANKAN, J. M. HUYGHE, M. R. DROST, J. D. JANSSEN and A. HUSON, *Int. J. Numer. Meth. Engng* (submitted).
[17] K. J. BATHE, *Finite Element Procedures in Engineering Analysis*, 1st edn. Prentice Hall, Englewood Cliffs, New Jersey (1982).
[18] TNO Building and Construction Research Delft, The Netherlands, *DIANA User's Manual: Linear Static Analysis*, Release 5.1, Vol. 1 (1993).
[19] TNO Building and Construction Research Delft, The Netherlands. *DIANA User's Manual: Non-linear Analysis*, Release 5.1, Vol. 4 (1993).
[20] C. L. TRESTIK and R. L. LIEBER, *J. Biomech. Engng* **115,** 225 (1993).
[21] P. H. M. BOVENDEERD, The mechanics of the normal and ischemic left ventricle during the cardiac cycle. PhD Dissertation, University of Limburg, Department of Biophysics (1990).
[22] P. A. J. B. M. HUIJING and R. H. ROZENDAL, *Introduction to Human Kinesiology* (Edited by R. H. ROZENDAL, P. A. J. B. M. HUIJING, Y. F. HEERKENS and R. D. WOITTIEZ), 5th edn, Chap. 5, pp. 199–274. Educaboek BV, Culemborg (1990) (in Dutch).
[23] O. HUDLICKA, K. R. TYLER, A. J. A. WRIGHT and A. M. A. R. ZIADA, *Skeletal Muscle Microcirculation; Proc. 3rd Bodensee Symp. Microcirculation* (Edited by F. HAMMERSEN and K. MESSMER), Number 5 in Progress in Applied Microcirculation, pp. 44–61. Karger, Basel (1984).
[24] J. Z. LIVINGSTON and J. R. RESAR, *Am. J. Physiol.* **265,** H1215 (1993).
[25] J. R. RESAR, R. M. JUDD, H. R. HALPERIN, V. P. CHACKO, R. G. WEISS and F. C. P. YIN, *Cardiovasc. Res.* **27,** 403 (1993).
[26] A. WISNES and A. KIRKEBØ, *Acta Physiol. Scand.* **96,** 256 (1976).

(Revision received and accepted 27 June 1995)